Catena 118 (2014) 154–167

Contents lists available at ScienceDirect

Catena

journal homepage: www.elsevier.com/locate/catena

Applied comparison of the erosion risk models EROSION 3D and LISEM for a small catchment in Norway

Torsten Starkloff *, Jannes Stolte

Norwegian Institute for Agricultural and Environmental Research, Soil and Environment Division, Fredrik A. Dahls vei 20, N-1432 Ås, Norway

ARTICLE INFO

Article history:
Received 28 February 2013
Received in revised form 31 January 2014
Accepted 9 February 2014

Keywords:
LISEM
EROSION 3D
Soil
Erosion
Modelling
Runoff

ABSTRACT

The loss of fertile soil from agricultural areas in Norway is especially harmful because of the thin layer of nutrient rich soil and the limited space where agriculture is possible. Physically based soil erosion prediction models have proved to be good tools to simulate and quantify soil erosion, but are not well established in Norway yet. Due to that this study was undertaken to further improve the knowledge about soil erosion development on agricultural areas and to better establish physically based models as an additional tool for soil research, in Norway. Two models were chosen for this study: the Limburg Soil Erosion Model (LISEM) and the EROSION 3D model. These two models were applied to the Skuterud catchment in the Ås municipality, for which measured discharge data, at the outlet, was available. The goal of this study was to investigate how the differences of two physically based models will influence the result of one and the same problem, to give an in-depth insight of what are the sources of uncertainty in modelling processes. To do that both models were calibrated by comparing the simulated hydrograph with the measured data. Special attention was given to the dependency of the model results on effects of grid cell size and time resolution. The grid cell size of the maps was easily adapted by using digital elevation models (DEM) obtained from airborne light detection and ranging (LIDAR) data. Furthermore the predicted erosion patterns were compared with an orthographic picture to validate the simulation results also in a spatial context.

With both models, it was possible to simulate a satisfactory accurate hydrograph and total amount of surface discharge. However, the output maps produced by the models showed quite different erosion and deposition features.

1. Introduction

In northern countries, erosion rates often follow a seasonal pattern with the highest soil losses during late autumn and early spring. For most of the total soil loss only a few runoff events are responsible each year (Lundekvam et al., 2003). The loss of fertile soil on agricultural areas in Norway is especially harmful because of the thin layer of nutrient rich soil and the limited space where agriculture is possible. Due to unfavourable conditions for agriculture in large parts of the country, only 3% (about 1 million ha) of the total land area of Norway is cultivated (Lundekvam et al., 2003). Soil erosion and flooding can cause major off-site damages. Studies in Belgium, for example, have estimated the mean annual cost of off-site damages caused by muddy floods to 14–140 million euros per year (Evrard et al., 2007). In addition to this it is expected that the extent, frequency and magnitude of soil erosion due to the change of rain fall intensity caused by climate change will increase (Pruski and Nearing, 2002; Deelstra et al., 2011).

It is important to understand the processes behind discharge development and soil erosion to combat negative impacts of extreme weather events. Besides field and laboratory investigation, physically based erosion risk models have proved to be good tools to understand these processes (e.g. Bhuyan et al., 2002; Boardman, 2006; Nearing et al., 2005). Furthermore, models can help to, e.g. quantify the impact of climate change and land use on soil and water quality, risk of water pollution by agrochemicals like nutrients and pesticides, flooding frequency and efficiency of mitigation measures.

Except for a few modelling attempts with empirical erosion models (e.g. Lundekvam, 2007), only a few studies have used physically based erosion prediction models to simulate erosion in Norway (e.g. Grønsten and Lundekvam, 2006; Kværnø and Stolte, 2012), yielding rather different results. Therefore, this study was undertaken to further improve the knowledge about soil erosion processes on agricultural areas in Norway and to better establish physically based models as an additional tool in soil science in Norway. Two models were chosen for this study: the Limburg Soil Erosion Model (LISEM) (De Roo et al.,

* Corresponding author. Tel.: +47 46932253.
E-mail address: torsten.starkloff@bioforsk.no (T. Starkloff).

http://dx.doi.org/10.1016/j.catena.2014.02.004

1996a, 1996b; Jetten, 2002) and the EROSION 3D model (Schmidt, 1996 and v. Werner, 2004). These models were chosen, for several reasons:

1. both models have been widely used in different studies, e.g. LISEM in Jetten et al. (1999), Takken et al. (1999), Hessel (2005), Hessel and Tenge (2008), Stolte et al. (2005), Hessel et al. (2003), Nearing et al. (2005), Hengsdijk et al. (2005), Sheikh et al. (2010), and EROSION 3D e.g. in v. Werner (1995), Schmidt and v. Werner (2000), Michael et al. (2005), Schob et al. (2006), Schindelwolf and Schmidt (2009), Köthe and Wurbs (2010);
2. to continue the evaluation of LISEM for Norway started by Kværnø and Stolte (2012);
3. to test the EROSION 3D model under the conditions of Norway. To evaluate if EROSION 3D and its parameter catalogue (DProc software), which was calibrated for a specific region (Saxony) in Germany (Michael, 2000), can be used without major changes in the different climate of South-Norway.

The main objective of this study was to compare results of two physically based models for calculating discharge and runoff:

(i) to give an in-depth insight of what the sources of uncertainty in the modelling process are, including the model design (i.e. process representation, equations used), to help users to choose the right model for the right purpose,
(ii) to analyse the effect of topographical data with different resolutions,
(iii) to quantify the influence of choices of initial and boundary conditions on modelling results.

Spatial erosion/deposition models should be validated in a spatial context and not only by a comparison of the outlet results (Takken et al., 1999). To do so we compared the produced soil loss maps of the two models with each other and with an orthographic picture.

2. Methodology

2.1. Study area

The study area was the Skuterud catchment located in Ås and Ski municipalities, approximately 30 km south of Oslo. The dominating land use is agriculture with cereal production – which covers approximately 60% of the catchment – followed by 33% pine forest and 7% urban area (Kværnø et al., 2007). The mean annual temperature is 5.3 °C and the mean precipitation is 785 mm per year. The catchment size is approximately 450 ha (4.5 km^2) and the altitude alters from 85 to 150 m above sea level. The topography can be characterized as undulating.

The soil maps provided by the Norwegian Forest and Landscape Institute (www.skogoglandskap.no) cover only the arable land. According to these maps the main soils in the central parts are marine silt loam and silty clay loam, classified after the World Reference Base for soil resources (WRB) as Albeluvisols and Stagnoslos. In the areas surrounding the central marine deposits, sand and loamy sand are predominating, classified as Cambisols, Arenosols, Umbrisols, Podzols and Gleysols.

For the calibration of the LISEM and EROSION 3D models a sub-catchment in the south eastern part of the main catchment (Fig. 1) was chosen. After recognising a high erosion risk within the sub catchment a monitoring station was installed at the outlet of the sub-catchment in 2008 (Kramer and Stolte, 2009). This station measures precipitation, runoff and soil loss continuously.

2.2. Models

Both models are physically based and work on a catchment scale, i. e. they use raster maps as input. These raster maps are created using geo-information-system (GIS) based software, ArcGIS (http://www.esri.com/software/arcgis (12.13.2012)) for EROSION 3D and PCRaster (http://www.pcraster.geo.uu.nl/ (12.13.2012)) for LISEM. Furthermore, both models are event based, which means they are used to predict soil erosion and surface discharge caused by short-term (few minutes up to a couple of days) rain events.

The major differences between the models are how they calculate infiltration, overland flow and soil detachment and deposition, which results in different sensitivity to changes in the input parameters and therefore in different calibration procedures as well as different results. The models are described in detail in Schmidt (1996) and v. Werner (2004), for EROSION 3D and De Roo et al. (1996a and 1996b) and Jetten (2002) for LISEM. A good overview about the differences and similarities of the two models was given by Boardman and Poesen (2006).

To simulate the infiltration and surface runoff, LISEM and ERSOSION 3D use different approaches. For the LISEM simulations, the Swatre sub-model (Belmans et al., 1983) was used in this study (Kværnø and Stolte, 2012). In the Swatre sub-model, infiltration and soil water flow in the soil profile are simulated by solving the Richard's equation. Soil hydraulic characteristics (i.e. water retention and (un-)saturated hydraulic conductivity) of each soil layer are needed, and can either be measured or predicted by using pedo-transfer functions.

The infiltration model used for EROSION 3D was developed by Schmidt (1993) and is based on the approach of Green and Ampt (Li et al. 1976). The infiltration rate is calculated with the Darcy equation (Schmidt, 1996). The Darcy equation contains variables which can be estimated (Ψ_m, K_s, θ_s) or measured (θ_i) (Schmidt, 1996). The matric potential (Ψ_m) of the soil for the initial moisture content (θ_i) is estimated with the equation of Van Genuchten and the saturated water content (θ_s) was estimated with the *p*edo-*t*ransfer-*f*unction (PTF) of Vereecken, whereas the saturated hydraulic conductivity (K_s) is estimated by the PTF of Campbell (Schmidt, 1996).

The basic concept of the spatial distribution for the overland flow is the same in the two models. Both models use a flow path model which is derived from the *d*igital *e*levation *m*ap (DEM) (Jetten, 2002, v. Werner, 2004). Furthermore, both models calculate the runoff velocity (v_q) using the approach of Manning-Stickler, as:

$$v_q = 1/n \times \delta^{(2/3)} \times S^{(3/5)} \quad (1)$$

where:

v_q	flow velocity [m s^{-1}]
n	Manning's n [s $m^{-1/3}$]
δ	hydraulic radius [m]
S	slope [–]

The hydraulic radius (δ) is calculated differently in LISEM and EROSION 3D due to the different approaches used to define the surfaces in each model's individual cells.

In LISEM one grid cell can have more than one type of surface as shown in Fig. 2. The infiltration characteristics vary according to the different surfaces in the grid cell, giving an individual water height above each surface type (Fig. 2). An average water height is then calculated for the grid cell, which results in an average hydraulic radius (δ_L; Eq. (2)) that is used to calculate the flow velocity (Eq. (1)).

$$\delta_L = A/P_w \quad (2)$$

where:

A	wet cross sectional area [m^2]
P_w	wet perimeter [m]

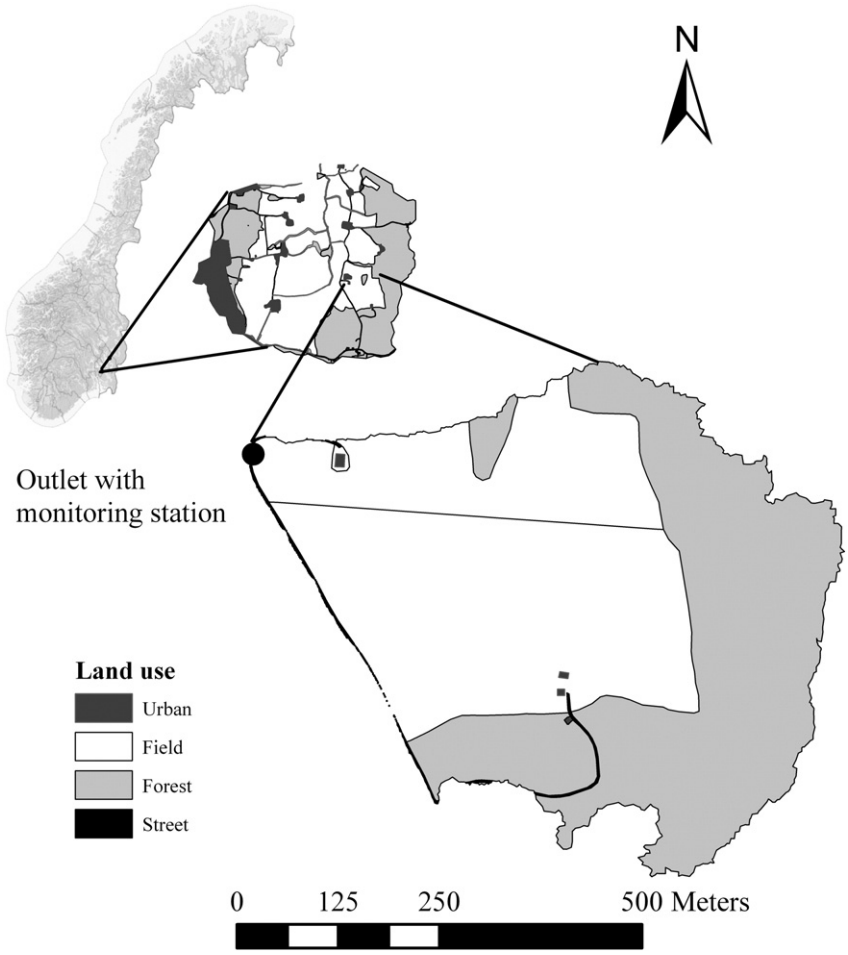

Fig. 1. Location of the Gryteland sub-catchment within the Skuterud catchment in Norway.

Using Eq. (3) for the wet cross section area (A) the discharge per cell Q_L [$m^3\ s^{-1}$] can be calculated:

$$A = \alpha \times Q_L{}^{\beta} \tag{3}$$

where:

α = $((n/s^{(1/2)} \times P_w)^{(2/3)})^{\beta}$
β 0.6.

In LISEM the channel and overland flow is calculated separately with separate kinematic waves. For the distributed overland and channel flow routing, a four-point finite-difference solution of the kinematic wave is used together with Manning's equation. The kinematic wave is done over the Local Drain Directions map that forms a network which connects cells in 8 directions (Jetten, 2002).

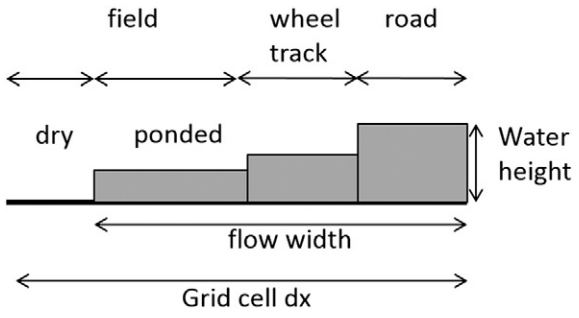

Fig. 2. Calculation of the average water height due to different surfaces in a grid cell of LISEM (Jetten, 2002).

The basic version of EROSION 3D does not take the kinematic wave into account (v. Werner, 2004). Later a sub-module was included into EROSION 3D with a simplification of the kinematic wave approach similar to LISEM, to improve the results for the discharge development over time (v. Werner, 2004). Different to LISEM, the approach of EROSION 3D uses a dynamic reservoir (M) for each grid cell which depends on the hydraulic radius (Eq. (6)) and the size of the gird cell.

$$M = \delta_R \times \partial x \tag{4}$$

where:

M storage capacity of the water film [m^3]
∂x area of the cell [m^2].

This dynamic reservoir will be filled as long as the runoff increases and starts to be emptied when the runoff starts to decrease. The resulting error in velocity is assumed to be small for relatively small catchments if a small time resolution (10 to 60 s) is chosen. An increasing error is expected in catchments with small slope angles due to the increasing diffusion and tailback of the surface water (for more details see v. Werner, 2004).

In EROSION 3D the discharge (Q_R) for each grid cell is calculated as follows:

$$Q_R = (r_a\text{-}i) \times \partial x + q_{in} \quad (5)$$

where:

Q_R discharge [$m^3\ s^{-1}$]
r_a precipitation intensity in relation to the slope angle [$mm\ min^{-1}$]
i infiltration rate [$mm\ min^{-1}$]
∂x grid cell length [m]
q_{in} inflow from other grid cells [$m^3\ s^{-1}$].

where Q_R is used to calculate the hydraulic radius (δ_R) (Eq. (6)), that is used to calculate the flow velocity (v_q) (Eq. (1)).

$$\delta_R = \left((Q_R \times n)/S^{(1/2)}\right)^{(3/5)} \quad (6)$$

For calculating soil detachment both models are using a combination of detachment processes. One process is the detachment of particles by rain drops and the second is the detachment by overland flow. Different approaches to calculate these processes are used in the models. In LISEM the amount of detached particles in the suspension (e) is a balance between the continuous counteracting processes of erosion and deposition (Dp), presented in Eq. (7). Where erosion is the sum of splash detachment by rain drops (Ds) and detachment by overland flow (Df).

$$e = Ds + Df\text{-}Dp \quad (7)$$

The detachment by rain drops in LISEM is related to the kinetic energy of the rainfall (Ke_r and Ke_t, Eq. (8)) which is the case for EROSION 3D as well (Eq. (14)), but different approaches are used in the models. In LISEM the kinetic energy of the rainfall (Ke_r and Ke_t) is calculated as follows:

$$Ke_r = 8.95 + 8.44 \times \log(\mathrm{Ri}) \text{ (free rain fall) and } Ke_t = 15.8 \times \left(h_p\right)^{(1/2)}\text{-}5.87 \text{ (through fall from plant canopy).} \quad (8)$$

Ri is the rainfall intensity ($mm\ h^{-1}$), h_p the plant height [m] and Ke in $J\ m^{-2}\ mm^{-1}$. Two different equations for calculating Ds can be used for LISEM depending on the values of Ke. But in general following Eq. (9) is used (Jetten, 2002):

$$Ds = ((2.82/As) \times Ke \times exp(\text{-}1.48 \times h) + 2.96) \times P \times A \quad (9)$$

where:

Ds splash detachment [$kg\ s^{-1}$]
As aggregate stability [–]
h depth of surface water layer [mm]
P precipitation (no plant cover) or through fall (with plant cover) in [mm]
A surface area over which splash takes place [m^2].

The flow detachment and deposition in LISEM are depending on the transport capacity (Tc) of the surface runoff (Eq. (10)):

$$Tc = \chi \times \left(s \times v_q \times 100\text{-}CSP\right) \times \varepsilon \quad (10)$$

where:

Tc transport capacity [$kg\ m^{-3}$]
$\chi =$ $((D50 + 5)/0.32)^{-0.6}$, where D50 is the median grain size [μm]
$\varepsilon =$ $((D50 + 5)/300)^{0.25}$
CSP critical stream power [$0.4\ cm\ s^{-1}$]
S slope [–].

If the transport capacity (Tc) is greater than the sediment concentration (Sc) in the flow, the flow detachment (Df) is calculated as follows:

$$Df = Y \times (Tc\text{-}Sc) \times Sv \times \partial t \times \partial x \times \delta \quad (11)$$

where:

Df flow detachment [$kg\ s^{-1}$]
Y efficiency coefficient
Sc sediment concentration [$kg\ m^{-3}$]
Sv settling velocity of the particle according to Stokes' law [$m\ s^{-1}$].

If the transport capacity (Tc) is smaller than the sediment concentration (Sc) deposition occurs.

In EROSION 3D the calculation of the detachment of particles depends on a dimensionless factor E (Erodibility), which is calculated as follows:

$$E = \left(\varphi_q + \varphi_r\right)/\varphi_{crit} \quad (12)$$

where:

φ_q momentum flux of the surface runoff [N]
φ_r momentum flux of rain drop impact [N]
φ_{crit} critic momentum flux of the soil [N].

This factor is used to determine when particles are detached from the soil. If $E > 1$ detachment of particles starts and if $E \leq 1$ the sum of the forces of overland flow and splash are not strong enough to detach particles and no erosion occurs.

The momentum flux of the surface runoff (φ_q) is calculated as follows:

$$\varphi_q = \left(Q_R \times p_q \times v_q\right)/\partial x \quad (13)$$

where:

p_q liquid density of water [$kg\ m^{-3}$]

and the momentum flux of rain drops (φ_r) is defined as follows:

$$\varphi_r = r_\alpha \times \partial x \times p_r \times v_r \times sin\ \alpha \times (1\text{-}C_L) \quad (14)$$

where:

r_α precipitation intensity in relation to the slope α [$m\ s^{-1}$]
p_r liquid density of the rain [$kg\ m^{-3}$]
v_r mean fall velocity of the rain drops [$m\ s^{-1}$], where $v_r = 4.5 \times \mathrm{Ri}^{0.12}$
α slope angle [°]
C_L canopy [%].

The critical momentum flux (φ_{crit}) gives an indication of the erosion resistance of the soil. It is determined by simulated rainfall experiments, where it is assumed that a minimum discharge (q_{crit}), which depends on the properties of the soil, is necessary to dispatch particles from the soil surface. With insertion of the minimum

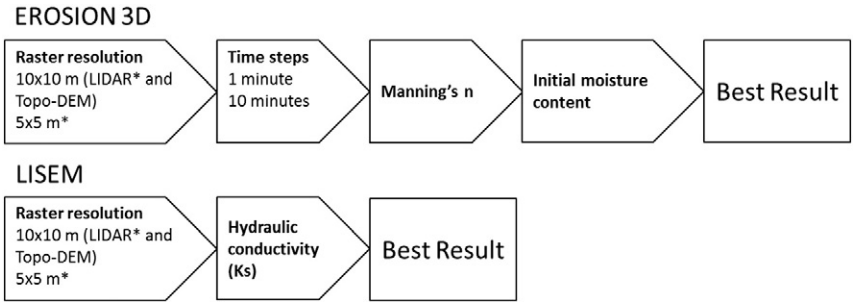

Fig. 3. Calibration scheme for the undertaken calibration for both models with the order of undertaken calibration steps (* unfiltered and filtered).

discharge (q_{crit}) into Eq. (13), the critical momentum flux (φ_{crit}) for a certain soil can be calculated (Eq. (15)).

$$\varphi_{crit} = \left(q_{crit} \times p_q \times v_q\right)/\partial x \tag{15}$$

The amount of detached particles which can be transported with the discharge depends, like in LISEM, on the transport capacity ($q_{s,max}$) of the surface discharge, but the transport capacity ($q_{s,max}$) of the surface discharge depends on two processes in EROSION 3D:

1. Deposition of particles due to gravity; and
2. The turbulent current working against this deposition. This turbulent current is a combination of the impulse forces of rain drops and overland flow.

The first process is similar to the LISEM approach (Eq. (11)) described by Stokes' law. By multiplication the value of the sinking velocity of Stokes' law and the mass flow as described in Schmidt (1996) the critical momentum flux of the flow ($\varphi_{q,crit}$) is calculated as follows:

$$\varphi_{q,crit} = c \times p_p \times \partial x^2 \times {v_p}^2 \tag{16}$$

where:

c	concentration of particles in the suspension [$m^3\ m^{-3}$]
p_p	density of the particles [$kg\ m^{-3}$]
v_p	sinking velocity [$m\ s^{-1}$].

If the momentum flux in the suspension is below $\varphi_{q,crit}$ the particle will sink to the ground.

The second process received no consideration in LISEM, but is in the EROSION 3D model implemented. The vertical turbulent momentum flux ($\varphi_{q,vert}$) is defined as:

$$\varphi_{q,vert} = 1/K \times \left(\varphi_q + \varphi_r\right) \tag{17}$$

where:

K	deposition coefficient [–].

According to that the surface runoff has reached its transport capacity when the vertical momentum flux is equal to the critical impulse force of the particles in the suspension.

$$\varphi_{q,vert} = \varphi_{q,crit} \tag{18}$$

Through insertion of Eqs. (16) and (17) into Eq. (18), it is possible to calculate the maximal concentration of dispatched particles c_{max} [$m^3\ m^{-3}$] in the discharge:

$$c_{max} = 1/K \times \left(\left(\varphi_{q,vert} + \varphi_{q,crit}\right)/\left(p_p \times \partial x^2 \times v_p\right)\right) \tag{19}$$

With which the transport capacity of the discharge can be calculated:

$$q_{s,max} = c_{max} \times p_p \times Q_R \tag{20}$$

where:

$q_{s,max}$	maximal transport capacity [$kg\ m^{-1}\ s^{-1}$].

2.3. The dataset

2.3.1. Calibration event

For the calibration of the models, a storm event on August 13, 2010 was chosen (Fig. 4). Precipitation was monitored at the same location as runoff, i.e. at the sub-catchment outlet, with a resolution of 1 min (Kværnø and Stolte, 2012). The event used in the model calibration had a duration of 12 h 50 min and yielded a total of 24.2 mm of precipitation.

2.3.2. Soil parameters

The soil maps for the LISEM input were available from the Norwegian Forest and Landscape Institute. This soil map covered the arable land only, with a coverage of approximately 94% (~6% of the arable land were not covered by the map), whereas no soil maps exist for the other land use types (forest, urban areas). To determine the soil types in the missing areas, a geological map was used and the soil type for forest and urban area was assumed to be loamy medium sand (Kværnø et al., 2007). From these soil textures the median texture coefficient (d_{50}) was calculated (Kværnø and Stolte, 2012). LISEM requires input of soil hydraulic tables (text files) containing data about (un-) saturated hydraulic conductivity and soil water retention as a function of matric potential, and maps with other parameter values. These maps include general catchment maps, land use and vegetation maps, soil surface maps, erosion maps, profile maps, and channel maps. All these maps were prepared by using a digital elevation model (DEM), a land use map, a soil map and a stream map. The soil properties, water retention, hydraulic conductivity, cohesion and aggregate stability, were calculated from textural composition and soil organic matter using pedotransfer-functions (Kværnø and Stolte, 2012).

The EROSION 3D model requires eight soil input parameters (Michael, 2001). The parameters' bulk density, initial moisture, erodibility, Manning's n, cover and skin factor were derived from a parameter catalogue which is included in the DProc software given the soil type, land use, season, soil cover, tillage practice and initial soil water level (v. Werner, 2010). To use the soil types from the LISEM input for the EROSION 3D model, the Norwegian soil types had to be translated into the German soil types. To determine the correlating German soil types, the KA-5 soil types (Ad-hoc-AG BODEN, 2005) were entered into the Norwegian soil texture triangle corresponding to their particle size percentages. At the time of the rain event in August 2010, the fields of the catchment had already been harvested and were covered with

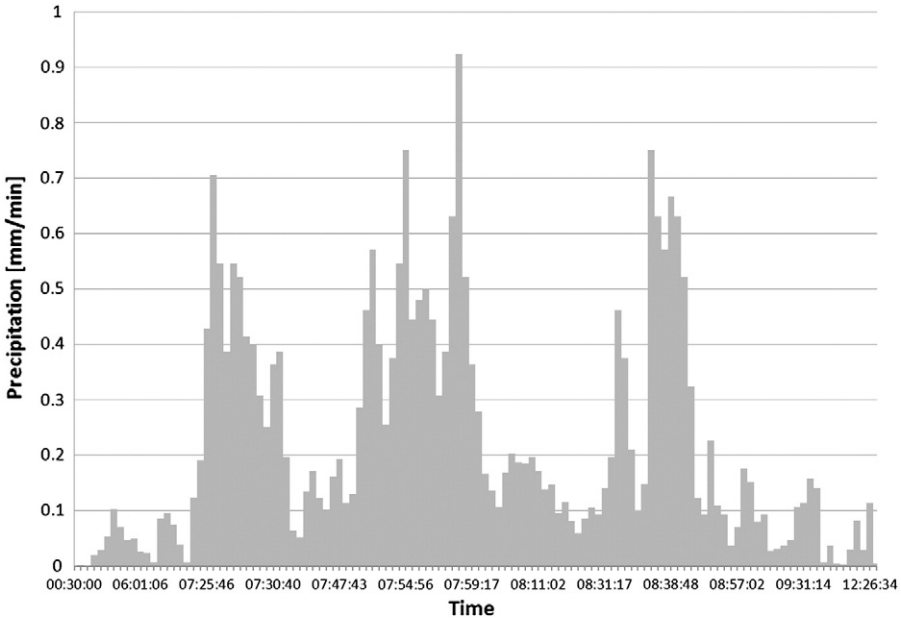

Fig. 4. Precipitation graph for the August 13, 2010 event.

stubble. For this type of land use, variations in tillage and season are not captured by the DProc software. Crop conditions were set to be on an average stock and the mulch content was set to 0%.

2.3.3. DEM generation

The "Topo-DEM" which was used by Kværnø and Stolte (2012) for the simulations with LISEM was derived from a topographic map, using the software ESRI/ArcMap 9.3; a grid cell size 10 ×10 m was used. This DEM was also used for one calibration approach taken with the EROSION 3D model (Fig. 7) to compare the results with LISEM.

The "LIDAR-DEMs" used in this study were generated from raw LIDAR-point clouds provided as LAS-files by the company BLOM, which obtained the point clouds through airborne based LIDAR. LIDAR — point clouds were used for creating the DEMs in this study because the high resolution of measurements (distance between points are less than 1 m) allows to create DEMs which present the natural terrain more accurate (Fig. 11) and lead to more realistic overland flow distribution (as discussed in Sections 4.2 and 4.3) compared to DEMs created from topographic maps. Furthermore, it is possible to easily create DEMs with high resolutions of up to 1 × 1 m.

Gaps in the DEM caused by filtering out vegetation etc. were closed by creating a *T*riangulated *i*rregular *n*etwork (TIN) from the point cloud with the software ESRI/ArcMap 10. In total, 4 DEMs were created, 2 filtered DEMs with the resolution 5 × 5 m and 10 × 10 m and 2 unfiltered DEMs with the same resolutions. The LIDAR DEMs were filtered with a low pass average filter (ArcMap-tool). The 10 × 10 m DEM was filtered one time and the 5 × 5 m DEM four times. The filtering was undertaken to remove wrong (e.g. short vegetation classified as bare soil) and missing data points which tended to occur most frequently in forest areas (due to vegetation) and led to an unrealistically rough surface (Köthe and Wurbs, 2010). The areas with inaccurately high roughness could lead to slower surface runoff velocities in simulations, giving less total

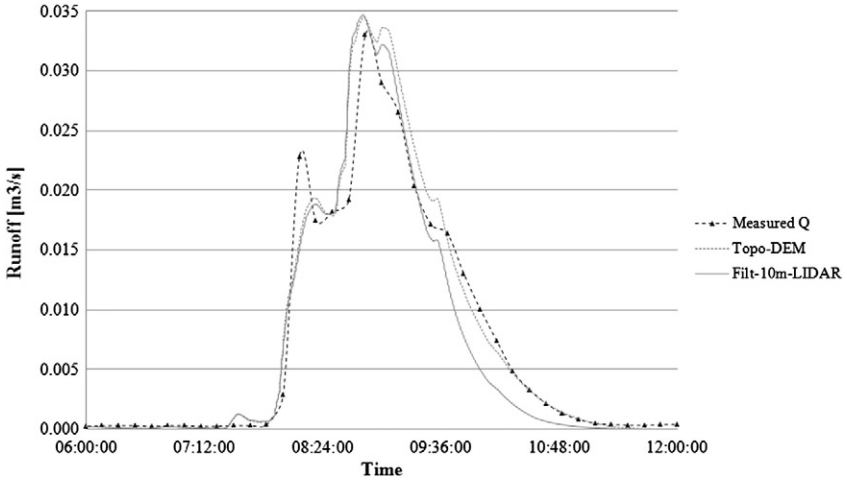

Fig. 5. Comparison of the hydrograph calculated with LISEM; with the Topo-DEM by Kværnø and Stolte (2012) and the 10 × 10 m filtered LIDAR-DEM, with the measured discharge.

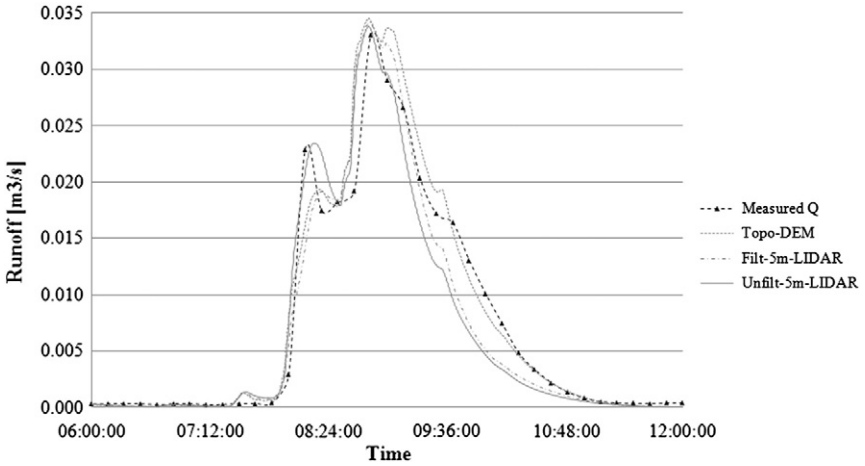

Fig. 6. Comparison of the hydrographs calculated by LISEM, with the Topo-DEM and the 5 × 5 m filtered and unfiltered LIDAR-DEM, with the measured hydrograph.

surface runoff (Köthe and Wurbs, 2010, v. Werner, 2004). This was investigated during the calibration of EROSION 3D with the 5 × 5 m LIDAR-DEM simulation approaches.

The grid sizes 10 × 10 m and 5 × 5 m were chosen for three reasons:

1. the 10 × 10 m grid size was chosen to compare the results of DEMs derived from topographic maps and LIDAR;
2. the 5 × 5 m grid size was chosen because the sub-catchment is only (approx.) 0.25 km^2, and because the general rule for the EROSION 3D model – to choose a time resolution of 1 min and a grid size of 10 × 10 m – only applies to catchment sizes of 1–10 km^2 (v. Werner, 2004); and
3. to investigate if the more detailed DEMs of 5 × 5 m can improve the model results in this study.

2.4. Calibration procedure

EROSION 3D is highly sensitive to Manning's n of the surface and the initial moisture content (v. Werner, 2004). Those two parameters were used for the calibration in this study. V. Werner (2004) also suggests that bulk density should be a calibrated value. After a couple of test runs we concluded that changing bulk density lead to no improvement in the accuracy of the results. For LISEM several studies (e.g. Hessel et al., 2003; Jetten et al., 1999) have shown that it is most sensitive to the parameters saturated conductivity (K_s) and initial matric potential. The initial matric potential was adjusted by Kværnø and Stolte (2012) and only the saturated conductivity (K_s) was used for the calibration in this study. In Fig. 3 a calibration scheme for the undertaken calibration of both models is illustrated.

2.4.1. Calibration of LISEM

The LISEM model (version 2.58) was calibrated for the sub-catchment, with the August 2010 event using measured surface runoff data, by Kværnø and Stolte (2012) (Fig. 5). A time resolution of 30 s was chosen with a total simulation period of 1000 min. A value of 0.01 was used for Manning's n in the channel and the initial pressure head was set to −5 kPa. For the simulation with the DEM derived from the topographic map, the Ks for the clay soil was multiplied by a factor of 4.51 in order to fit the simulated hydrograph to the measured graph. An overview of the used input parameters for the LISEM calibrations is shown in Table 1.

For the simulations with the filtered 10 × 10 m LIDAR-DEM, the same multiplication factor of 4.51 for the K_s of the clay soils, as used by Kværnø and Stolte (2012), was employed. Only small adjustments had to be done when LISEM was used with the filtered 5 × 5 m LIDAR-DEM. To fit the simulated hydrograph to the measured graph the K_s had to be multiplied with 4.515. For the test runs with the 5 × 5 m unfiltered LIDAR-DEM the K_s for the clay soils was multiplied by 4.9.

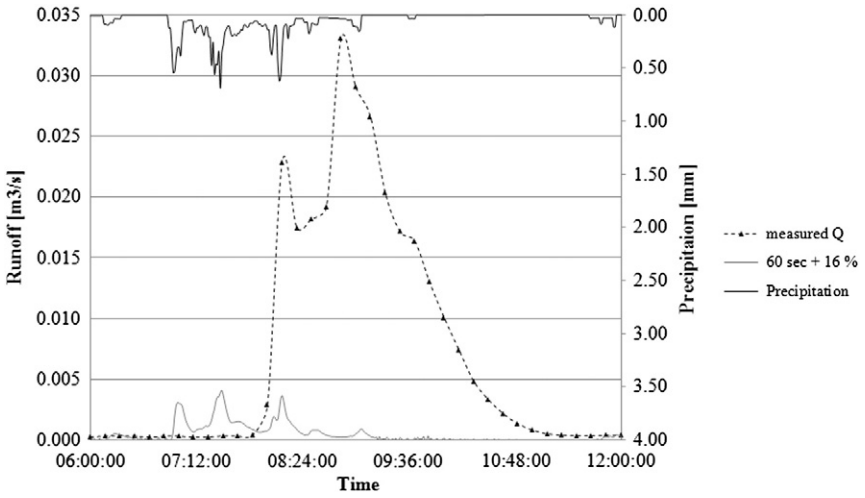

Fig. 7. Observed rainfall and measured discharge and surface discharge calculated with EROSION 3D with the Topo-DEM.

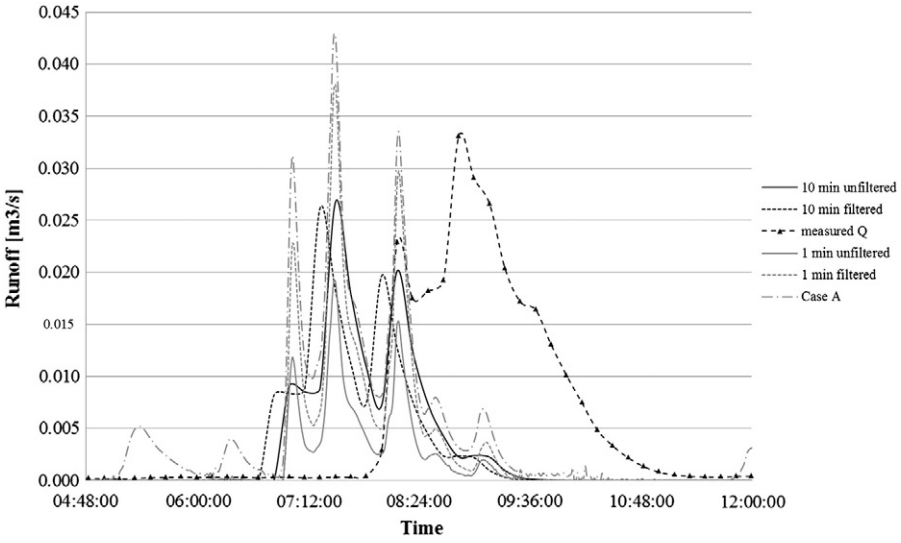

Fig. 8. Hydrographs calculated with the filtered and unfiltered 10 × 10 m LIDAR-DEMs for a 10 min and a 1 min time-resolution compared with the measured hydrograph. The curve "Case A" represents the simulation approach with 16% greater initial moisture content for all land use types (filtered DEM with 10 min time-resolution).

2.4.2. Calibration of EROSION 3D

To calibrate the EROSION 3D model (version from 2011) a one-dimensional sensitivity analysis was taken, as recommended by v. Werner (2004). This approach assumes that the model's predicted results are linear dependent on the input parameters. In this study the focus was on the following interactions:

- The influence of the soil parameters: Manning's n (only for the agricultural land use) and initial moisture (for all land use types) on the surface runoff prediction; and
- The influence of the grid size and calculation time step of the simulation on the surface runoff prediction.

The results of the different analyses were compared with the measured runoff values from the sub-catchment outlet. A selection of important input parameters for the different soil types are shown in Table 2.

3. Results

3.1. LISEM calibration

As for the calibration with the Topo-DEM, the hydrograph of the calibration result with the filtered 5 × 5 m LIDAR-DEM fits rather well with the measured hydrograph. The hydrograph closely follows the shape of the hydrograph calculated with the topographic map (Fig. 5). Both curves have the same start time for discharge and also the end-times correspond closely. Only small differences can be observed after the second peak. The third peak of the hydrograph calculated with the LIDAR-DEM is slightly smaller than the one calculated with the Topo-DEM. Furthermore, the peak discharge is slightly smaller than the peak of the Topo-DEM-calibration. This resulted in a smaller amount of total discharge (Table 3).

The hydrograph for the LISEM calibration with the unfiltered 5 × 5 m LIDAR-DEM fits the measured graph in shape as well as in size (Fig. 6).

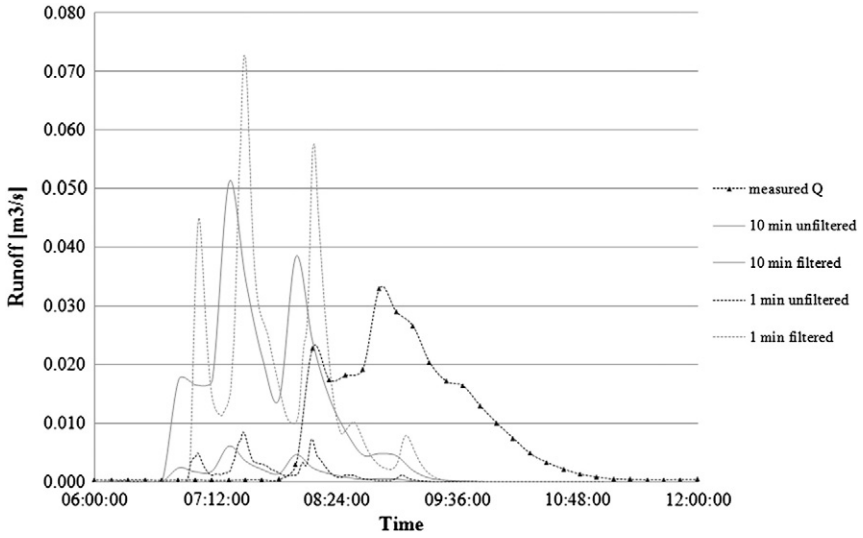

Fig. 9. Hydrographs calculated with EROSION 3D with the filtered and unfiltered 5 × 5 m LIDAR-DEMs for a 10 min and a 1 min time-resolution compared with the measured hydrograph.

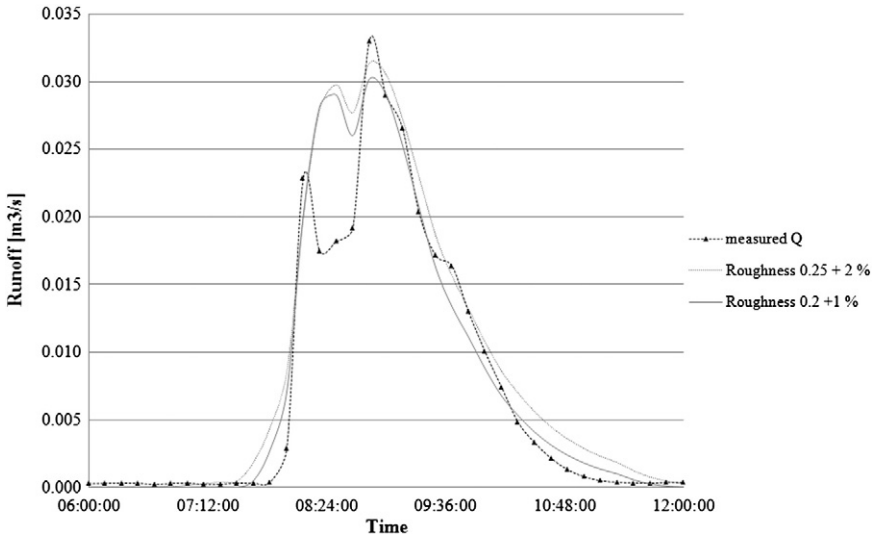

Fig. 10. Hydrographs for the two best calibration results with EROSION 3D with the filtered 5 × 5 m LIDAR-DEM (roughness = Manning's n).

Compared to the other two calculated graphs the first peak of the measured hydrograph was better simulated, but similarly to the graph for the filtered LIDAR-DEM (5 × 5 m), the graph is smaller than the measured hydrograph, which results in a smaller total runoff (Table 3).

3.2. EROSION 3D calibration with the Topo-DEM

The hydrograph by EROSION 3D with the Topo-DEM did not fit the measured hydrograph (Fig. 7); EROSION 3D produced an approximately one magnitude lesser surface discharge. The calibration with 16% higher initial moisture provided the best result (Fig. 7). This increase of the initial moisture content was required to bring the input value closer to the value which was used for the LISEM calibration (Table 1). The initial matric hydraulic head for the LISEM input was −50 cm, which, using the soil water retention curve, leads to an approximate increase of 16% of the values given from the DProc programme (Table 2). Nonetheless the shape of the modelled hydrograph is considerably different than the measured hydrograph; following the distribution of the rain event more closely. These characteristics could not be modified substantially by introducing changes in time resolution, initial moisture content or surface roughness (Manning's n).

3.3. EROSION 3D calibration with the LIDAR-DEMs

Fig. 8 shows the modelled hydrograph using the 10 × 10 m LIDAR-DEMs and the two different time resolutions (10 min and 1 min).

The predicted hydrograph for the filtered DEM was slightly larger than the predicted hydrograph for the unfiltered DEM, both for time resolutions of 10 min and 1 min, while the predicted hydrograph for the 1 min time resolution was not significantly larger than predicted with a 10 min time resolution. To increase the amount of surface runoff for the 10 min time resolution, the calibration approach that used 16% higher initial moisture content, than generated by DProc (Table 2), was applied (Fig. 8, Case A), giving a larger predicted peak discharge (the maximum discharge rate was over 0.03 $m^3 s^{-1}$). However the early signs of numerical instability can be seen, especially between 04:48 h and 07:00 h. The same approach was done by using a 1 min time resolution which also produced higher runoff, but showed some degree of numerical instability.

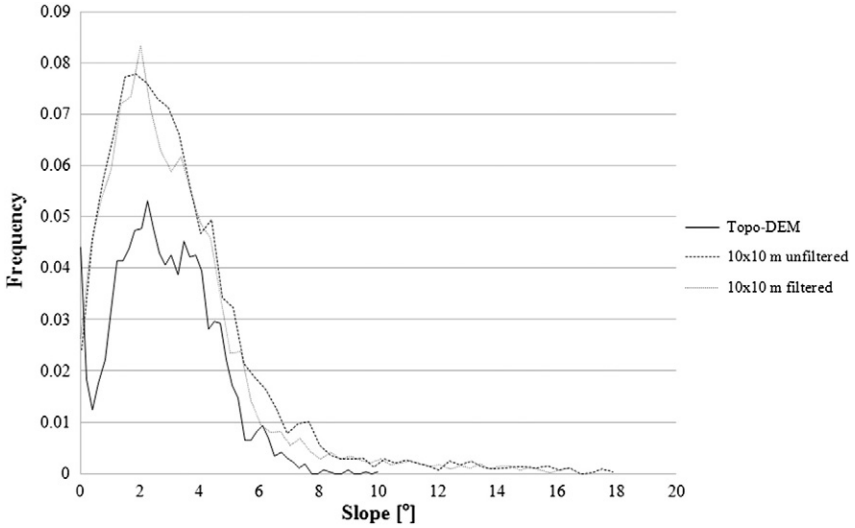

Fig. 11. The frequency of different slope angles per gird cell in the filtered and unfiltered 10 × 10 m LIDAR-DEMs and the Topo-DEM.

Table 1
Input parameters for the LISEM calibrations (changed after Kværnø and Stolte, 2012.

Parameter	Stream	Urban	Forest	Arable
Channel cohesion [kPa]	15,000	–	–	–
Channel Manning's n [s $m^{-1/3}$]	0.01	–	–	–
Channel wide [m]	1	–	–	–
Slope of channel sides [°]	45	–	–	–
K_s [cm d^{-1}]	–	81.6	81.6	Variable
Initial matric potential [cm]	–	−50	−50	−50
Random roughness [cm]	–	0.8	3.2	0.88
Manning's n [s $m^{-1/3}$]	–	2.4	1.2	0.6
Fraction of soil covered by vegetation [–]	–	0.9	0.9	1
Vegetation height [m]	–	0.2	7	0.7
Leaf area index [–]	–	1.5	6	2.5
d50 value of the soil [μm]	–	50	50	50
Cohesion of bare soil [kPa]	–	20	20	Variable
Additional cohesion by roots [kPa]	–	5	10	1
Aggregate stability [–]	–	66	66	Variable

Further calibration by changing the values for surface roughness and initial moisture achieved no further improvement of the predicted hydrographs, but showed decreasing numerical stability with increasing roughness values. Less numerical instability was observed in simulations with the unfiltered DEM than those with the filtered DEM.

The simulations with different time resolutions produced substantially different results with the 5×5 m unfiltered and filtered LIDAR-DEMs. Fig. 9 presents the results of the simulation with 1 min and 10 min time resolutions. The predicted surface discharge obtained using the unfiltered DEM was substantially smaller than the predicted surface discharge of the filtered DEM. As with the predicted surface discharge obtained using the 10 × 10 m DEMs, the predicted surface discharge with the 1 min time resolution was slightly larger than those with the 10 min resolution. The 1 min results were not used for further calibration as they showed signs of numerical instability (between 08:36 h and 09:36 h).

After calibrating the value for the surface roughness (Manning's n) – arriving at two values, 0.2 and 0.25 s $m^{-1/3}$ which gave hydrographs with similar shapes as the measured graph – the initial moisture was slightly adjusted to increase the amount of surface discharge. The best results were achieved with an increase of the initial moisture content by 1–2% depending on the value of Manning's n (1% for a Manning's n of 0.25 s $m^{-1/3}$, and 2% for a Manning's n of 0.2 s $m^{-1/3}$). But for all simulation cases, an earlier start of surface discharge was observed, approximately 50 min earlier than what was measured in the field.

Both results showed two peaks, which were observed in the measured runoff (Fig. 10), but the first peak in each case was approximately 0.005 m^3 s^{-1} larger than that of the measured surface discharge, and their maxima occurred approximately 10 min later than that of the measured case (after offsetting the simulated hydrographs by 50 min to fit to the measured graph, for better comparison (Fig. 10)). The two calibration results predicted a slightly larger total surface discharge volume than the measured data (Table 4), whereas the total surface discharge for the simulation with 1% increased initial moisture correlated more closely with the measured surface discharge. Additionally, one simulation was carried out with the same values for Manning's n and initial water content, which were used for the LISEM calibration (Manning's n 0.6 s $m^{-1/3}$ and initial moisture increased by +16%). The result was still in the same order of magnitude, but the two peaks which were characteristic of the measured surface discharge were no longer distinguishable and the simulated surface discharge ended much later (20:30 h) than that which was measured.

Table 2
Input parameters for the EROSION 3D calibration (selection).

Parameter	Field 1	Field 2	Forest	Urban
Soil type (German)	Lu	Sl3	Sl3	Sl3
Bulk density [kg m^{-3}]	1540	1600	1000	1370
C_{org} [%]	1.5	1	5	2.7
Initial moisture [vol.%]	36	25	34	34
Erodibility [N m^{-2}]	0.008	0.009	0.1	0.002
Manning's n [s $m^{-1/3}$]	0.015	0.015	0.9	0.9
Canopy [%]	90	90	100	90
Skin factor [–]	0.35	1	20	10

Table 3
Comparison of the calculated (EROSION 3D) and measured total discharge.

Simulation runs	Total calculated discharge	Measured total discharge
Topo-DEM	5.75 m^3	5.62 m^3
Filt-10 m-LIDAR	5.10 m^3	5.62 m^3
Filt-5 m-LIDAR	5.04 m^3	5.62 m^3
Unfilt-5 m-LIDAR	4.94 m^3	5.62 m^3

4. Discussion

4.1. LISEM

An explanation for why an increase imposed to K_s is justifiable in the procedure we followed, was offered by Kværnø and Stolte (2012). K_s is based on data using the Mualem–van Genuchten equations, which do not take macropore flow into account. However, as observed in the field, clay soils, in particular the Albeluvisols, can be highly macroporous and thus a greater effective value for K_s can be expected than the matrix K_s value. After adjusting the K_s, the calculated hydrographs for the simulation with the DEM derived from the topographic map and the DEMs derived from the LIDAR data, fitted rather well to the measured graph. Differences between the filtered and unfiltered DEMs, in case of the LIDAR-DEMs, had no large influence on the simulation results. The multiplication factor for the K_s of the clay soils did not differ much, only by 0.4 between the test runs with the filtered and unfiltered 5 × 5 m LIDAR-DEM, and not at all between the calibrations with the topographic DEM and the 10 × 10 m LIDAR-DEM. In a relatively plain agricultural landscape, with small changes in terrain between small distances, the change in resolution between 10 and 5 m has no large influence on the runoff character of the catchment. However, some influence of using a rougher surface was expected at least in the test runs with the unfiltered 5 × 5 m LIDAR-DEM due to larger vegetation-related errors in the LIDAR, but the data showed otherwise (Fig. 6). The simulation time (with an Intel® Core™ 2 Duo CPU P8700 at 2.53 GHz) increased, however, from about 10 min (filtered DEM) to 30 min (unfiltered DEM).

4.2. EROSION 3D

The simulations with the LIDAR-DEMs produced substantially different results depending on the grid size, slope (filtered vs. unfiltered) and time resolution. Some of the differences in these results were caused by the properties of the DEMs, and some by the surface runoff approach taken by EROSION 3D itself.

The numerical instability which was observed in results obtained using the 10 × 10 m DEMs was a result of the inappropriateness of this grid size for such a small catchment area. As shown by v. Werner

Table 4
Comparison of the calculated (EROSION 3D) and measured total discharge between 00:00 and 13:50.

Simulation runs	5 × 5 m filtered DEM	Measured surface discharge
Manning's n 0.25 + 2%	6.63 m^3	5.62 m^3
Manning's n 0.2 + 1%	5.90 m^3	5.62 m^3

(2004), for a 1–10 km^2 catchment a grid size of 10 m is recommended. The calibration area in this study was ~0.25 km^2 in size, and as a result the runoff velocity increased because of the increasing runoff amount per grid cell (Eq. (5)) and the excessive smoothing of the surface (decrease of slope angle). This issue can be explained by looking at Eqs. (1), (6) and (4) in the runoff module for EROSION 3D, where the hydraulic radius (δ_R) depends on the slope angle (Eq. (6)). As a result, the runoff velocity (v_q) (Eq. (1)) and capacity of the water film (M) (Eq. (4)) are strongly associated with the slope angle. To investigate whether the 10 m DEMs contain a high number of grid cells with small slope angles the ArcMAP — tool "slope" was applied to measure the slope angles (Fig. 11).

For both DEMs most slope angles for each grid cell were between 1° and 4°, which indicates a very flat surface. Such flat surfaces result in increased runoff velocities and discharge per cell which could lead to a numerical instability in the runoff prediction (v. Werner, 2004).

The calibration approach with the 5 × 5 m DEMs showed substantially better results compared to the 10 × 10 m DEMs. However problems did occur, especially when the 1 min time resolution was used. The predicted discharge for both time resolutions (1 and 10 min) for the unfiltered 5 × 5 m DEM was much smaller compared to the predicted discharge of the filtered DEM (Fig. 12), which was a result of the rougher surface in the unfiltered DEM. In the unfiltered DEM all the classification errors from the LIDAR processing, like vegetation, tillage rills etc. behaved like barriers (Köthe and Wurbs, 2010) which increased for example the length of the flow path. Filtering the DEM five times proved to be adequate to remove classification errors in the LIDAR data and create a DEM which was smooth enough to show a realistic runoff pattern. By considering the hydrographs (Fig. 10) and the predicted runoff volumes for the filtered DEMs (Table 4), a grid size of 5 × 5 m was necessary to give a satisfactory simulation approach for the sub-catchment. The observed differences in the start and ending time of the simulated surface discharge compared to the measured runoff could have had several causes. V. Werner (2004) observed that by increasing the raster resolution, the predicted runoff starts and ends earlier. Furthermore, the complete modelling of detailed water movement with velocity changes and kinematic wave are not included in the approach taken by EROSION 3D to simulate water runoff (v. Werner, 2004). Therefore not all factors that influence the surface water flow and that may delay the start of measurable surface discharge at the catchment outlet were taken into account. Nonetheless, the predicted hydrographs in Fig. 10 give a good approximation of the measured surface discharge — the form of the graphs shows similar characteristics to those of the measured surface discharge (both peaks exist).

4.3. Comparison of the calibration results of LISEM and EROSION 3D

The simulation results obtained using EROSION 3D with the DEM which was used for the LISEM modelling, correlated poorly with the measured runoff (Fig. 7). To investigate if the DEM itself caused the poor simulation results, the slope angles of each grid cell were examined. As is evident in Fig. 11, the investigation showed that the Topo-DEM featured a flatter relief than the 10 × 10 m LIDAR DEMs.

According to v. Werner (2004) a flatter relief leads to numerical instability in the predictions made by the EROSION 3D model. The Topo-DEM contained a number of 0° slope values, whereas the LIDAR-DEMs had a minimum slope angle of 0.134° (Fig. 11). The small slope angle values in the Topo-DEM grid cells produced very slow runoff velocities and low water storage capacities for the water film, which can be explained by Eqs. (4), (8) and (9), where

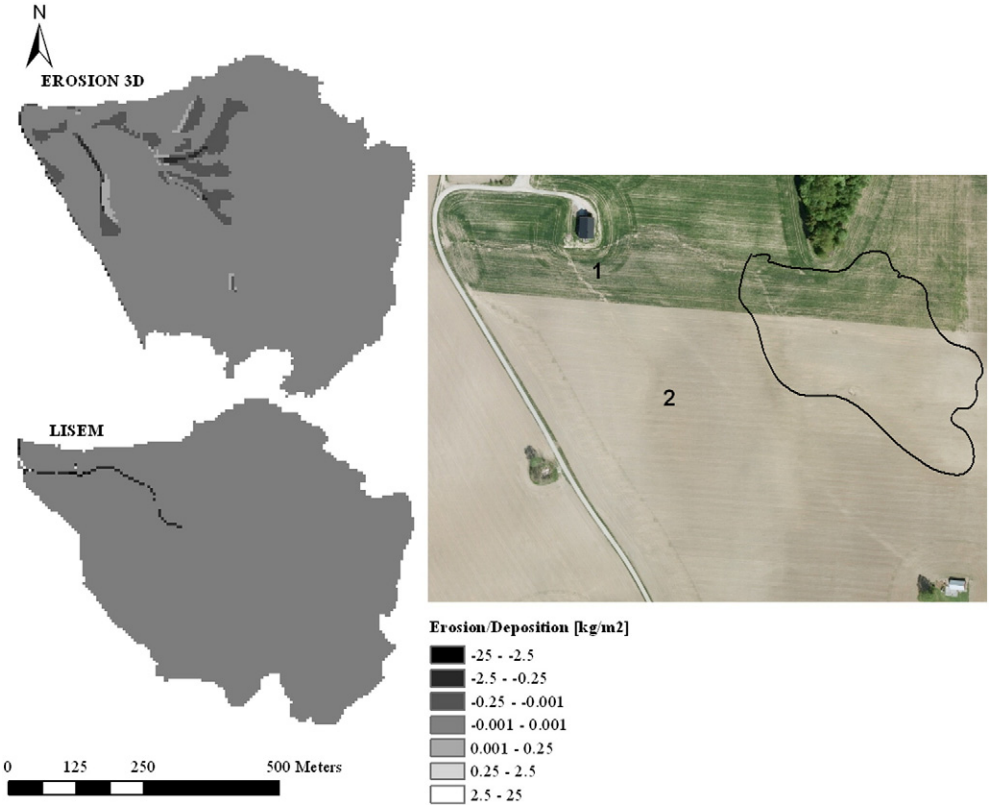

Fig. 12. Comparison of the soil-loss-maps provided from LISEM and EROSION 3D with an orthographic picture of the sub-catchment (www.norgeibilder.no, date of picture: 05.13.2008).

a value of zero for the slope angle always produces results of zero. Of course a subroutine is included in EROSION 3D which prevents zero values for the flow velocity, but nonetheless the predicted amount of surface runoff will be substantially smaller than the measured surface discharge in these cases.

There are several possible reasons for the LISEM calibration results fitting the measured runoff characteristics better (Fig. 5), despite the mentioned errors in the DEM:

- Instead of calculating only the surface runoff, the total discharge is calculated as combination of surface runoff, which drains into the channel and the channel runoff itself;
- A different approach for calculating the overland flow is applied in LISEM than in EROSION 3D; and
- A different infiltration module is used in LISEM than in EROSION 3D.

For the LISEM calibration, the runoff produced from channel cells was used. The water from the overland flow usually drains into the channel cells and then flows to the outlet of the catchment (Jetten, 2002). Such channel formation by the eroding forces of surface water runoff was observed in the selected catchment. To allow a better comparison of the results, the channel runoff was simulated with EROSION 3D as well. However, the peak discharge (0.14 $m^3 s^{-1}$) was significantly larger than the peak discharge of the measured surface discharge (0.033 $m^3 s^{-1}$). This discrepancy between results produced by LISEM and EROSION 3D originated from the second of the reasons presented above: the different approaches taken in the calculation of overland flow. First, the approach taken by EROSION 3D was not considered and recommended for use in simulating channel runoff since it does not properly represent the geometry and runoff resistance of the channel (v. Werner, 2004). Second, the simplified approach in EROSION 3D, is much more exposed to changes in time and spatial resolution (Table 6). The more sophisticated approach in LISEM makes it less dependent on time resolution, which the user can freely change independently from the time resolution of the input precipitation file (Table 6). Furthermore the spatial resolution of the DEM of a relatively uniform catchment has a smaller influence on the simulation results of LISEM. The different approaches taken to calculate infiltration were another point of difference which can lead to significantly different runoff results. This indicated the change of the K_s for the clay soil by multiplying it with 4.51 during the LISEM calibration (Kværnø and Stolte, 2012), whereas initial moisture and Manning's n are the calibration values used by EROSION 3D. The total discharge for the three different simulations is presented in Table 5, where there were no substantial differences between the results of LISEM and EROSION 3D. The simulated hydrographs of LISEM and EROSION 3D fitted the measured graph well, but while LISEM underestimated the first peak, EROSION 3D overestimated the first peak.

4.4. Spatial comparison

For the spatial comparison of the model results of LISEM and EROSION 3D, the 5 × 5 m filtered LIDAR DEM was chosen, because EROSION 3D only showed satisfactory results with this DEM. For LISEM, the simulation with a multiplication factor of 4.515 for the K_s (Fig. 6), and for EROSION 3D, the simulation with a Manning's n of 0.2, and an initial moisture increase by 1% (Fig. 10) was chosen. The orthographic photo for the catchment was available at the web page www.norgeibilder.no (12.14.2012). Unfortunately, no pictures were available for the modelled event (08.13.2010). The only available picture was from 05.13.2008. Due to that the following comparison is only qualitative and it should be kept in mind that the produced map by LISEM may fit better to the actual modelled event.

Table 5
Comparison of measured and calculated total amount of surface discharges.

EROSION 3D	LISEM	Measured runoff
5.90–6.63 m^3	4.94–5.75 m^3	5.62 m^3

Where EROSION 3D directly delivers a map with the erosion and deposition values, LISEM (vers. 2.58) provides two maps, one with the erosion values and one with the deposition values. To get the sediment budget the cell values of the two maps were summed up. The results for the spatial distribution of soil erosion and deposition are quite different for the two models (Fig. 12). Where LISEM only predicted erosion/deposition in the channel which was predefined (marked with number 1 in the picture), the erosion/deposition map delivered by EROSION 3D shows a much more diverse distribution of erosion and deposition patterns. Compared with the orthographic picture of the catchment, EROSION 3D predicted the observed erosion/deposition structures better than LISEM. The marked area in the picture as well as the second channel (marked with number 2 in the picture), can be seen in the map provided by EROSION 3D. It was not possible to distinguish between structures caused by deposition and structures caused by erosion in the picture. However, the comparison showed that the two models produced rather different erosion and deposition maps, even though they calculated the same amount and time distribution of discharge. One reason for the differences is most likely the inclusion of channel flow in the LISEM model, where most of the soil loss is produced in the simulation. Soil loss from the EROSION 3D model has to come from the surface, since channel erosion is not included in these runs. A test run without the channel was performed for the LISEM model which produced almost no runoff and no erosion. Furthermore, the models calculate deposition and erosion quite different as presented in Section 2.2, which probably results in different erosion/deposition patterns as well. However, in both models the flow velocity has an important role for the amount of flow detachment (e.g. see Eqs. (10), (11), (13), (15), (16), (19)), which is strongly influenced by the Manning's n of the soil surface. By looking at Tables 1 and 2 it can be seen that different Manning's n for the agricultural areas were used. For LISEM a much higher Manning's n (0.6 s $m^{-1/3}$) was chosen compared to EROSION 3D (0.015 s $m^{-1/3}$). Only for the channel a comparable Manning's n of 0.01 s $m^{-1/3}$ was used, which can explain why LISEM only produced erosion in the channel in this study. To investigate this a test run with LISEM, where the channel was switched off and Manning's n for the fields was set to the value of the best calibration result with EROSION 3D (0.025 s $m^{-1/3}$) was performed, which produced similar erosion/deposition patterns as EROSION 3D but the simulated hydrograph was not comparable anymore (14.33 m^3 modelled total runoff at the outlet vs. 5.62 m^3 measured total runoff).

5. Conclusion

With both models it was possible to simulate a satisfactory accurate hydrograph and total amount of surface discharge in the sub-catchment for the 2010 rain event. Therefore, it can be concluded that both LISEM and EROSION 3D can be used as tools to predict and locate areas with erosion risk. However, this conclusion does have some limitations.

(1) The land use type for agricultural land was “stubbles” in this study. This land use type, which was used as an input for the DProc software, is independent from the season in the year and tillage. Due to that, further tests should be done to examine if the input parameters for different land use types and for different seasons and tillage practices provided by the DProc software can be used in Norway. (2) This conclusion only applies to areas with characteristics similar to the Skuterud catchment. For areas in Norway with other characteristics in relief, soil properties and climate, further validation has to be undertaken to test the two models under these conditions. (3) The influences of snow cover and soil freezing (important factors in the Norwegian environment) on the prediction capability of the models, have not been taken

Table 6
Overview of the undertaken simulation runs and the final values of the calibration parameters (grey: calibration run with the best simulated surface discharge using EROSION 3D; LISEM gave for all four calibrations satisfying results).

Parameters	Topo–DEM		LIDAR–DEMs 10x10 m					LIDAR–DEMs 5x5m					
			Unfiltered		Filtered			Unfiltered			Filtered		
	L	E	E	E	E	E	L	E	E	L	E	E	L
Time steps [sec]	30	60	600	60	600	60	30	600	60	30	600	60	30
K_s [cm d^{-1}] (*	4.51	–	–	–	–	–	4.51	–	–	4.9	–	–	4.515
Manning's n [s $m^{-1/3}$]	–	–	–	+0.05; +0.1	–	+0.05; +0.1	–	–	–	–	–	+0.2; +0.25	–
Initial moisture content [%]	–	–	–	+16%	–	+ 16%	–	–	–	–	–	+1%; +2%	–

into account in this study, and must therefore be investigated further. Furthermore, the comparison of the calibration procedure of the two models showed that EROSION 3D has problems to properly predict the surface discharge with the implemented approach to calculate the development of the surface runoff. To calibrate EROSION 3D with measured surface discharge is rather time consuming and includes several difficulties for the user to find the correct calibration values. To get to a satisfying result in this study, several parameters had to be adjusted (Table 6). During the calibration of the EROSION 3D model in the subcatchment, it was observed that the process of finding the correct grid size and time resolution for such small catchments is not easy and requires experience. To gain realistic hydrographs for small catchments (<1 km^2), a raster resolution of 5 × 5 m or higher (e.g. 3 × 3 m) is required.

Instead, LISEM easily adapted the different raster resolutions and the results were relatively independent from the roughness of the different DEMs (filtered or not) in this study. Only the simulation time increased, although not as much as for EROSION 3D. Furthermore, the results of LISEM were independent from the time resolution of precipitation data. LISEM gave a much better prediction of runoff behaviour in channels, probably due to the infiltration approach taken in the Richard equation and a better estimation of the kinematic wave in channels and rills. To verify this conclusion, (1) a simulation with the Green and Ampt approach in LISEM should be undertaken, and (2) simulations with EROSION 3D using the multiple-layer-infiltration-extension should be tried, as that could produce better results, and was also observed in different studies (e. g. Seidel, 2008; Schindelwolf and Schmidt, 2009). This approach could not be undertaken in this study because it requires a considerable amount of measured input data which was not available at the time.

On the other hand, EROSION 3D requires a relatively small amount of measured input data (if Green and Ampt infiltration module is used), compared to LISEM, which results in a decrease of operational hours to collect this data. EROSION 3D is therefore a good planning tool, while LISEM is probably the better choice for investigation of hydrological processes in a catchment.

The differences in the produced erosion/deposition maps showed that the model results do not only have to be compared with outlet measurements, but also with detailed field investigations of the spatial distribution of erosion and deposition patterns. Only with the exact knowledge where and to which amount soil loss and sedimentation took place in the catchment, a more valid comparison and validation of the performance of models can be done. In this study the spatial comparison of the results showed that even if the simulated hydrographs show good results it doesn't necessarily mean that the modelled erosion and deposition are correct. Especially if estimated input parameters are used (e.g. Manning's n) the user has to be aware that the choice of parameters for the calibration can have a strong effect on the performance of the model and the produced results. As Stroosnijder (2005) indicated it is recommended to measure as many parameters as possible in the field for limiting the uncertainties during the simulation and calibration procedure.

References

Ad-hoc-AG BODEN, 2005. Bodenkundliche Kartieranleitung, 5 Aufl. Hannover.
Belmans, C., Wesseling, J.G., Feddes, R.A., 1983. Simulation model of the water balance of a cropped soil: SWATRE. J. Hydrol. 6, 271–286.
Bhuyan, S.J., Kalita, P.K., Janssen, K.A., Barnes, P.L., 2002. Soil loss predictions with three erosion simulation models. Environ. Model Softw. 17, 137–146.
Boardman, J., 2006. Soil erosion science: reflections on the limitations of current approaches. Catena 68, 73–86.
Boardman, J., Poesen, J., 2006. Soil Erosion in Europe. John Wiley & Sons Ltd, England.
De Roo, A.P.J., Wesseling, C.G., Ritsema, C.J., 1996a. LISEM: a single event physically-based hydrologic and soil erosion model for drainage basins: I. Theory, input and output. Hydrol. Process. 10, 1107–1117.
De Roo, A.P.J., Offermans, R.J.E., Cremers, N.H.D.T., 1996b. LISEM: a single event physically-based hydrologic and soil erosion model for drainage basins: II. Sensitivity analysis, validation and application. Hydrol. Process. 10, 1119–1126.
Deelstra, J., Øygarden, L., Blankenberg, A.B., Eggestad, H.O., 2011. Climate change and runoff form agricultural catchments in Norway. lim. Chang. Strateg. Manag. 3 (4).
Evrard, O., Bielders, C.L., Vandaele, K., v. Wesemael, B., 2007. Spatial and temporal variation of muddy floods in central Belgium,off-site impacts and potential control measures. Catena 70, 443–454.
Grønsten, H.A., Lundekvam, H.E., 2006. Prediction of surface runoff and soil loss in southeastern Norway using the WEPP Hillslope model. Soil Tillage Res. 85, 186–199.
Hengsdijk, H., Meijerink, G.W., Mosugu, M.E., 2005. Modeling the effect of three soil and water conservation practices in Tigray, Ethiopia. Agric. Ecosyst. Environ. 105, 29–40.
Hessel, R., 2005. Effects of grid cell size and time step length on simulation results of the Limburg soil erosion model (LISEM). Hydrol. Process. 19, 3037–3049.
Hessel, R., Tenge, A., 2008. A pragmatic approach to modelling soil and water conservation measures with a catchment scale erosion model. Catena 74, 119–126.
Hessel, R., Jetten, V., Baoyuan, L., Yan, Z., Stolte, J., 2003. Calibration of the LISEM model for a small Loess Plateau catchment. Catena 54, 235–254.
Jetten, V., 2002. LISEM, Limburg Soil Erosion Model, User's Manual. University of Utrecht.
Jetten, V., De Roo, A., Favis-Mortlock, D., 1999. Evaluation of field-scale and catchment-scale soil erosion models. Catena 521–541.
Köthe, R., Wurbs, D., 2010. Analyse des digitalen Geländemodells DGM2 für die Erosionsbewertung. ÖA LfULG, Schriftenreihe, Heft XX/2010.
Kramer, G.J., Stolte, J., 2009. Cold-season hydrologic modeling in the Skuterud catchment. An Energy Balance Snowmelt Model Coupled with a GIS-based Hydrology Model. Bioforsk Report, 4(126), p. 46. ISBN: 978-82-17-00548.
Kværnø, S.H., Stolte, J., 2012. Effects of soil physical data sources on discharge and soil loss simulated by the LISEM model. Catena 97, 137–149.
Kværnø, S.H., Haugen, L.E., Børresen, T., 2007. Variability in topsoil texture and carbon content within soil map units and its implications in predicting soil water content for optimum workability. Soil Tillage Res. 95, 332–347.
Li, R., Stevens, M.A., Simons, D.B., 1976. Solutions to the Green and Ampt infilttration equation. J. Irrig. Drain. Div. 2, 239–248.
Lundekvam, H.E., 2007. Plot studies and modelling of hydrology and erosion in southeast Norway. Catena 71, 200–209.
Lundekvam, H.E., Romstad, E., Øygarden, L., 2003. Agricultural policies in Norway and effects on soil erosion. Environ. Sci. Pol. 6, 57–67.
Michael, A., 2000. Anwendung des physikalisch begründeten Erosionsprognosemodells EROSION 2D/3D — Empirische Ansätze zur Ableitung der Modellparameter. (PhD Thesis) TU Bergakademie Freiberg.

Michael, A., 2001. Anwendung des physikalisch begründeten Erosionsprognosemodells EROSION 2D/3D — empirische Ansätze zur Ableitung der Modellparameter. Freiberg. Forschungsh. 488.
Michael, A., Schmidt, J., Enke, W., Deutschländer, T., Malitz, G., 2005. Impact of expected increase in precipitation intensities on soil loss — results of comparative model simulations. Catena 61, 155–164.
Nearing, M.A., Jetten, V., Baffaut, C., Cerdan, O., Couturier, A., Hernandez, M., Bissonnais, Y. Le, Nichols, M.H., Nunes, J.P., Renschler, C.S., Souche're, V., van Oost, K., 2005. Modeling response of soil erosion and runoff to changes in precipitation and cover. Catena 61, 131–154.
Pruski, F.F., Nearing, M.A., 2002. Climate-induced changes in erosion during the 21st century for eight U.S. locations. Water Resources Research 38.
Schindelwolf, M., Schmidt, W., 2009. Prüfung und Validierung des neu entwickelten Oberflächenabflussmoduls des Modells EROSION 3D im Zusammenhang mit Maßnahmen des vorsorgenden Hochwasserschutzes auf landwirtschaftlich genutzten Flächen. Schriftenreihe des Landesamtes für Umwelt, Landwirtschaft und Geologie, Heft 15/2009.
Schmidt, J., 1993. Teilmodell zur Simulation der Infiltration. Zwischenbericht zum BMFT-Vorhaben 0339233.
Schmidt, J., 1996. Entwicklung und Anwendung eines physikalisch begründeten Simulationsmodells für die Erosion geneigter landwirtschaftlicher Nutzflächen. Berl. Geogr. Abh. (61), 1–148.
Schmidt, J., v. Werner, M., 2000. Modeling sediment and heavy metal yields of drinking water reservoirs in the Osterzgebirge region of Saxony (Germany). In: Schmidt, J. (Ed.), Soil Erosion — Application of Physically Based Models. Berlin, Heidelberg, New York.
Schob, A., Schmidt, J., Tenholtern, R., 2006. Derivation of site-related measures to minimise soil erosion on the watershed scale in the Saxonian loess belt using the model EROSION 3D. Catena 68, 153–160.
Seidel, N., 2008. Untersuchung der Wirkung verschiedener Landnutzungen auf Oberflächenabfluss und Bodenerosion mit einem Simulationsmodell. (PhD Thesis) TU Bergakademie, Freiberg.
Sheikh, V., van Loon, E., Hessel, R., Jetten, V., 2010. Sensitivity of LISEM predicted catchment discharge to initial soil moisture content of soil profile. J. Hydrol. 393, 174–185.
Stolte, J., Ritsema, C.J., Bouma, J., 2005. Developing interactive land use scenarios on the Loess Plateau in China, presenting risk analyses and economic impacts. Agric. Ecosyst. Environ. 105, 387–399.
Stroosnijder, L., 2005. Measurement of erosion: is it possible? Catena 64, 162–173.
Takken, I., Beuselinck, L., Nachtergaele, J., Govers, G., Poesen, J., Degraer, G., 1999. Spatial evaluation of a physically-based distributed erosion model (LISEM). Catena 37, 431–447.
v. Werner, M., 1995. GIS-orientierte Methoden der digitalen Reliefanalyse zur Modellierung von Bodenerosion in kleinen Einzugsgebieten. (PhD Thesis) Freie Universität Berlin.
v. Werner, M., 2004. Abschätzung des Oberflächenabflusses und der Wasserinfiltration auf landwirtschaftlich genutzten Flächen mit Hilfe des Modells EROSION 3D. GeoGnostic, Endbericht, Berlin.
v. Werner, M., 2010. Data base — processor user manual. GeoGnostic Software Ver. 1.80, Berlin.